FULL PAPER

Dalton
www.rsc.org/dalton

Silver complexes of 1,1′,3,3′-tetrakis(pyrazol-1-yl)propane: the "quadruple pyrazolyl embrace" as a supramolecular synthon †

Daniel L. Reger,* James R. Gardinier, Radu F. Semeniuc and Mark D. Smith
Department of Chemistry and Biochemistry, University of South Carolina, Columbia, South Carolina 29208, USA. E-mail: reger@mail.chem.sc.edu

Received 10th February 2003, Accepted 12th March 2003
First published as an Advance Article on the web 2nd April 2003

The reaction between pyrazole and malonaldehyde bis(dimethylacetal) yields the first linked bis(pyrazolyl)methane ligand, $CH_2[CH(pz)_2]_2$. Reaction of this ligand with $Ag(O_3SCF_3)$ yields $[Ag_2\{\mu\text{-}CH_2[CH(pz)_2]\}_2](SO_3CF_3)_2$ (**1**). In the solid state **1** contains a dimeric dication in which two ligands sandwich two silver cations forming a bicyclic sixteen-membered ring system. A similar reaction with $Ag(NO_3)$ yields a trimetallic complex $[Ag_3\{\mu\text{-}CH_2[CH(pz)_2]_2\}_2](NO_3)_3(CH_3CN)_2$ (**2**) that crystallizes from acetonitrile as **2·CH$_3$CN**. Both **1** and **2** form supramolecular structures dominated by cooperative π–π stacking/CH–π hydrogen bonding interactions that we term the 'quadruple pyrazolyl embrace.' A Cambridge Structural Database search showed that this interaction is relatively common for metal complexes of simple poly(pyrazolyl)-methane or -borate ligands and occurs in a quarter of all cases.

Introduction

In light of the growing importance of coordination network solids,[1] bi- and multi-functional Lewis acids in supramolecular chemistry[2] and in catalysis,[3] the development of structurally-adaptive ligands, compounds that are capable of multiple binding modes to metal centers (chelating, bridging, or both modes simultaneously) and that are capable of becoming involved in multiple noncovalent interactions, would be highly desirable. To this end, our group has been interested in the preparation and reactivity of species that incorporate two or more poly(pyrazolyl)methane ligating sites that are bridged by either flexible or semi-rigid organic backbones. With metal complexes of the $C_6H_{6-n}[CH_2OCH_2C(pz)_3]_n$ (n = 2, 4) series of ligands, which are prototypical examples of semi-rigid organic-linked tris(pyrazolyl)methanes, the tripodal[4] κ^3, the bidentate[5] κ^2, and bridging bidentate/monodentate[6] κ^2–κ^1 binding modes have been observed. The propensity of the polar N-based heterocycles to become involved in π–π stacking as well as CH–π and other weak hydrogen bonding interactions has lead to the discovery of substances with unusual solid state supramolecular architectures.[4–6] While examples of organic-linked mono(pyrazolyl)methanes and their metal complexes are known,[7] there is a distinct absence of reports describing the preparation and chemistry of linked bis(pyrazolyl)methanes. In this contibution, a synthetic route to the first of a series of linked bis(pyrazolyl)methane compounds developed in our laboratories and two corresponding silver complexes are described. Furthermore, as a means of simplifying the future description of the noncovalent interactions that give rise to the supramolecular architectures observed in the title silver and numerous other metal complexes of poly(pyrazolyl)methane ligands, we introduce the concept of and detail the geometric parameters associated with the 'quadruple pyrazolyl embrace'– a concerted set of noncovalent interactions between a pyrazolyl tetrad that is reminiscent of the 'parallel quadruple phenyl embrace' as first described by Dance's group (Fig. 1).[8]

Results and discussion

The compound $CH_2[CH(pz)_2]_2$ (L) was prepared by the alcohol elimination reaction between pyrazole and commercially available malonaldehyde bis(dimethylacetal), as in eqn. 1.

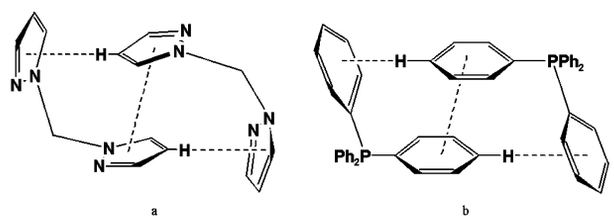

Fig. 1 A comparison between the structural motifs of a) the quadruple pyrazolyl embrace and b) the parallel quadruple phenyl embrace.

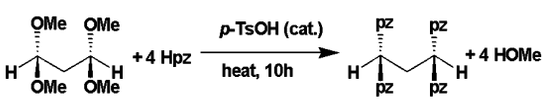

This reaction was essentially complete in ten hours as evidenced by the volume of methanol collected. Further heating caused some decomposition and a lower isolated yield. The results obtained by monitoring the reaction progress by NMR spectroscopy implicated the known acid-catalyzed formation of vinyl alkoxides from diacetals as a competing reaction.[9]

The reaction between $CH_2[CH(pz)_2]_2$ and $Ag(O_3SCF_3)$ in a 1 : 1 mol ratio in THF results in the precipitation of a colorless solid that analyzed as a compound with the empirical formula $[Ag\{CH_2[CH(C_3H_3N_2)_2]_2\}](O_3SCF_3)$, [Ag(L)](OTf). Its ESI(+) mass spectrum displayed signals for a dimeric unit corresponding to the $[Ag_2(L)_2(OTf)]^+$ cation along with peaks for monometallic $[Ag(L)]^+$ and $[Ag(L)_2]^+$ species. As expected from the lability of silver pyrazolyl complexes, the ^{1}H and ^{13}C NMR spectra showed only one set of resonances that are shifted downfield from those of the free ligand and the ^{19}F NMR contained only one resonance.

Slow diffusion of Et_2O into either acetone or acetonitrile solutions of this solid yields crystals of $[Ag_2\{\mu\text{-}CH_2[CH(pz)_2]\}_2](SO_3CF_3)_2$ (**1**), as shown by an X-ray structural investigation (Fig. 2). Two linked bis(pyrazolyl)methane ligands act in a bridging bidentate manner bonding two silver cations forming a dimeric unit, as suggested from the ESI(+) mass spectral data, rather than forming a coordination polymer.[4a,6] The coordination environment about silver is distorted tetrahedral owing to the small bite angles of 84.91(8)° and 82.57(8)° of the chelate rings and the asymmetric nature of the Ag–N bonds [three shorter bonds of 2.230(2), 2.285(2), 2.320(2) Å associated

† Electronic supplementary information (ESI) available: two possible representations of the coordination sphere about Ag(2a) in **2·CH$_3$CN**. See http://www.rsc.org/suppdata/dt/b3/b301635h/

DOI: 10.1039/b301635h

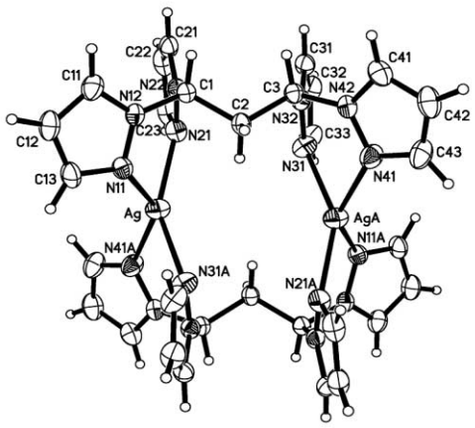

Fig. 2 Structure of the dication in $[Ag_2\{\mu\text{-}CH_2[CH(pz)_2]\}_2](SO_3CF_3)_2$ (**1**).

with N(21), N(41), and N(31), respectively, as well as one longer bond of 2.449(2) Å for Ag–N(11)]. Each silver center serves as a spiroatom that fuses two six-membered AgN_4C heterocylic rings that adopt a distorted boat conformation. Both sets of spirofused heterocyclic rings are connected *via* their carbon atoms by methylene units and form a central bicyclic sixteen-membered ring system where the interatomic separation between silver centers is 4.32 Å. A related homobimetallic derivative $\{Ag_2[(pz)(CH_2)_3]_2\}(NO_3)_2$ with a metal–metal distance of 5.334(1) Å has been reported.[7b]

As with the manganese[4c] and rhenium[4d] tricarbonyl complexes of linked tris(pyrazolyl)methane ligands, the extended structure of $[Ag_2(L)_2](OTf)_2$ contains intercationic π–π and CH–π interactions involving pyrazolyl groups (blue and red dashed lines, respectively, in Fig. 3) that organize the dications into polymeric chains that propagate along the *b* axis. Of the eight pyrazolyl groups in the dication, four participate in these intercationic stacking interactions. Of these, the pyrazolyl group that contains either N(21) or N(21a) of one dication is involved in a coplanar π–π stacking interaction with its respective symmetry-related counterpart [N(21a) or N(21)] of another dication [blue line Fig. 3; centroid–centroid distance 3.57 Å, ⊥ interplane separation 3.44 Å, slip angle, β = 15.7°]. The pyrazolyl groups are aligned such that the heteroatoms are in the energetically favorable head-to-tail arrangement. Each of these pyrazolyl groups also acts as a hydrogen donor in a CH–π interaction [red line Fig. 3; C(22)–H(22) ··· centroid angle of 142.6° and calculated H–centroid distance 2.69 Å] with a hydrogen-accepting pyrazolyl group that contains either N(11) or N(11a) (as dictated by the symmetry of the interaction). The geometry of each of these intercationic interactions is well within the accepted ranges.[10,11]

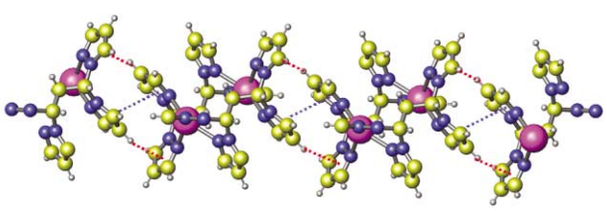

Fig. 3 View of the polymeric chain of cations in $[Ag_2\{\mu\text{-}CH_2[CH(pz)_2]\}_2](SO_3CF_3)_2$ formed by interactions between pyrazolyl groups.

The two pyrazolyl groups that contain N(21) and N(31), respectively, have an *intra*cationic centroid–centroid separation of 3.44 Å and a ⊥ interplane separation of only 3.32 Å. However, since the dihedral angle between the mean planes of these pyrazole rings is rather large (α = 19.5°) and the pyrazolyl groups are aligned such that the heteroatoms overlap any *intra*cationic stacking interaction involving these two rings would likely be repulsive in nature and/or simply a consequence of the crystal packing. Finally, the triflate counter anions reside between the chains of cations and, unfortunately, are disordered such that a discussion of any weak interactions that involve these groups is precluded.

The only product obtained from the reaction between $CH_2[CH(pz)_2]_2$ and $Ag(NO_3)$ in CH_3CN after 30 min of mixing followed by either removing solvent or precipitation with Et_2O and filtration was a compound with the formula $[Ag_3\{CH_2[CH(C_3H_3N_2)_2]_2\}_2](NO_3)_3(CH_3CN)_2$, **2**, as indicated by elemental analyses. This product, with a 2 : 3 mol ratio of ligand to metal, was obtained in quantitative yield regardless of the stoichiometry of reagents (ligand to metal mol ratios of 1 : 1 and 1 : 2 were utilized and the yield was based on the appropriate amount of limiting reagent). The complex is soluble in DMSO, CH_3CN, sparingly soluble in hot acetone, and insoluble in most other common organic solvents. The electrospray mass spectrum had signals corresponding to the trimetallic $[Ag_3(L)_2(NO_3)_2]^+$ fragment along with signals for the bimetallic $[Ag_2(L)_2(solvent)]^+$ and the monometallic $[Ag(L)]^+$, $[Ag(L)(CH_3CN)]^+$ and $[Ag(L)_2]^+$ species.

Slow diffusion of Et_2O into acetonitrile solutions of $[Ag_3(\mu\text{-}CH_2[CH(pz)_2]_2)_2](NO_3)_3(CH_3CN)_2$ afforded colorless crystals that were suitable for single crystal X-ray diffraction. The structure showed a remarkable trimetallic, tri-acetonitrile complex $\{Ag_3(\mu\text{-}CH_2[CH(pz)_2]_2)_2(CH_3CN)(NO_3)_3\}\cdot(CH_3CN)_2$, **2·CH$_3$CN** (Fig. 4). There are three types of silver centers within the complex; however, disorder due to 50% site occupancy of one coordinated acetonitrile and one bidentate nitrate anion renders two of the silver sites crystallographically indistinguishable. The structure depicted in Fig. 4 represents one of the two crystallographically superimposed species and will be used for further description. The central silver atom Ag(1) resides on the crystallographically imposed (false) C_2 axis and has a distorted tetrahedral coordination environment as a result of the 86.52(9)° bite angle for N(11)–Ag(1)–N(21) of the bis(pyrazolyl)methane chelate and the disparity in Ag–N bond lengths [2.274(2) Å for Ag(1)–N(21) and 2.345(3) Å for Ag(1)–N(11)]. A second distorted tetrahedral silver site is found which contains a $Ag(2)N_3O$ kernel as a result of the chelation of the bis(pyrazolyl)methane ligand and coordination of both a unidentate nitrate anion and an acetonitrile molecule. Within this kernel, the smallest angle in the distorted tetrahedral coordination sphere is associated with N(41)–Ag(2)–N(31) of the chelate ring which is 85.0(1)°. The corresponding Ag–N bond distances are 2.348(3) Å and 2.388(3) Å for Ag(2)–N(41) and Ag(2)–N(31), respectively. The largest angle of the distorted tetrahedron of 120.1(8)° occurs between O(1)–Ag(2)–N(51). The Ag(2)–O(1) distance of 2.401(3) Å is comparable to the distances found in another silver complex with unidentate

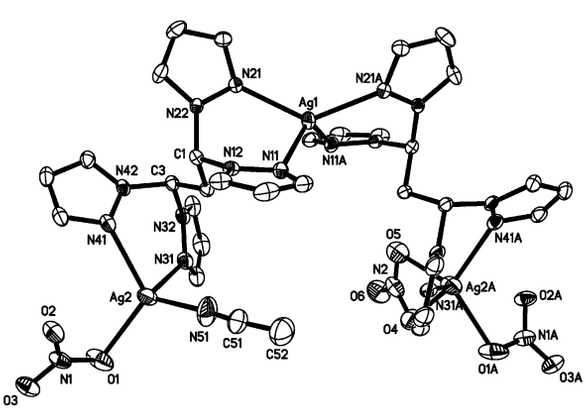

Fig. 4 View of one of the two superimposed trimetallic species from the crystallographic study of $[Ag_3(\mu\text{-}CH_2(pz)_4)_2(CH_3CN)(NO_3)_3]\cdot(CH_3CN)_2$, **2·CH$_3$CN**.

nitrate anions,[7b] and the Ag(2)–N(51) bond distance of 2.51(2) Å for the coordinated acetonitrile is longer than those of the pyrazolyl nitrogen atoms but is otherwise unremarkable. The third silver center is penta-coordinated as a result of the replacement of a coordinated acetonitrile molecule in the second type of silver site for a bidentate nitrate anion. The coordination environment about this five-coordinate third silver center can best be described as intermediate between a distorted square pyramid and a distorted trigonal bipyramid. In this case, the smallest angles in the $Ag(2a)N_2O_3$ core occur between O(4)–Ag(2a)–O(5), the bite angle of the bidentate nitrate anion [53.1(5)°], between O(1)–Ag(2)–O(5), the atoms of the two types of nitrate anions [74.9(2)°], and between N(31)–Ag(2a)–N(41) of the bispyrazolyl fragment [85.0(1)°]. The largest angle of 150.5(2)° occurs between O(4)–Ag(2a)–N(41) and all other bond angles lie in the range between 102° and 122°. Further details of the coordination environment are provided as ESI.†

As with the triflate counterpart, cooperative π–π and CH–π interactions involving pyrazolyl groups (blue and red dashed lines, respectively, in Fig. 5) associate the trimetallic 'cationic centers' of the nitrate complex in the solid state. These cooperative interactions occur between the pyrazolyl groups bound to the central silver site [Ag(1)] and assemble the 'cationic centers' into chains in the direction of the crystallographic *c* axis. The two pyrazolyl groups that contain N(11) and N(11a) are involved in π–π stacking interactions in which each pyrazolyl of one 'trication' stacks in a coplanar head-to-tail arrangement with the same type of pyrazolyl group of an adjacent 'trication' [blue dashed line Fig. 5; centroid–centroid distance 3.59 Å, ⊥ interplane separation 3.44 Å, slip angle, β = 16.6°]. These pyrazolyl groups also serve as hydrogen donors in CH–π interactions (red dashed lines, Fig. 5) with those hydrogen-accepting pyrazolyl groups that contain either N(21) or N(21a) where the C(12)–H(12) ··· centroid angle is 136.9° and the calculated H–centroid distance is 3.00 Å. The geometries of both types of interactions are comparable to those observed in the triflate derivative.

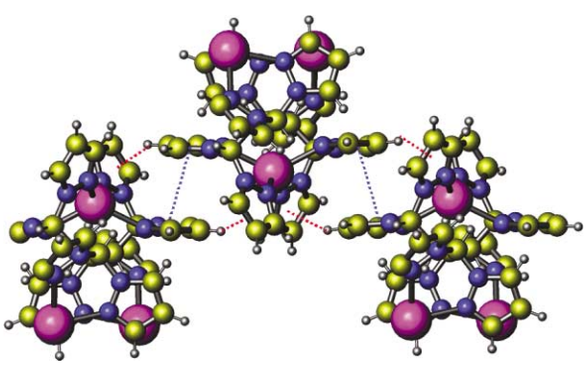

Fig. 5 View of cations in **2·CH$_3$CN** down the *a* axis emphasizing cooperative π–π (blue dashes) and CH–π (red dashes) interactions.

A bifurcated CH–π interaction[12] associates the chains of trimetallic units into a two-dimensional sheet as shown in Fig. 6. This interaction occurs between the hydrogens bound to C(22) (located at the 4-position of the 'donor' pyrazole ring labeled **pz$_1$** in Fig. 6) and the two pyrazolyl groups that contain N(31a), **pz$_{2a}$**, and N(41a), **pz$_{3a}$**, respectively, which act as acceptors. The C(22)–H(22) ··· centroid distances and angles are 3.125 Å, 120.4° for the part of the interaction involving **pz$_{2a}$** and 2.796 Å, 136.1° for that of **pz$_{3a}$**. The sum of the angles about H(22) is 348.2°. An equivalent bifurcated interaction between **pz$_{1a}$**, **pz$_2$** and **pz$_3$** is generated by the crystallographic symmetry.

The combination of the bifurcated CH–π interactions along with the cooperative π–π and CH–π interactions results in the organization of the 'cationic centers' into a columnar network as in Fig. 7. The nitrate anions and both coordinated and uncoordinated solvent molecules reside within the channels created by the pyrazolyl stacking interactions. The oxygen atoms of the unidentate nitrate anions are involved in a number of close contacts with the hydrogen atoms of the ligand. The distances and geometries of these interactions are given in Table 1 and are within the values suggested to indicate weak hydrogen-bonding interactions[12] and therefore may further support the structure of the columnar network.

Table 1 Details of weak hydrogen bonding interactions in **2·CH$_3$CN**

D–H ··· A	H ··· A/Å	D ··· A/Å	D–H ··· A/°
C(1)–H(1) ··· O(2)	2.40	3.33(1)	154
C(3)–H(3) ··· O(1)	2.47	3.36(1)	149
C(3)–H(3) ··· O(3)	2.44	3.36(1)	153
C(13)–H(13) ··· O(3)	2.45	3.31(1)	150
C(31)–H(31) ··· O(3)	2.51	3.26(1)	135
C(41)–H(41) ··· O(1)	2.31	3.10(1)	140

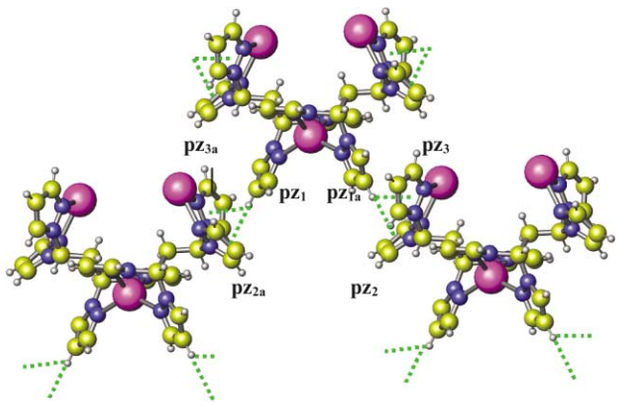

Fig. 6 View of the cations in **2·CH$_3$CN** along the approximate *c* axis emphasizing the bifurcated CH–π interactions (green dashed lines) between adjacent 'trications'.

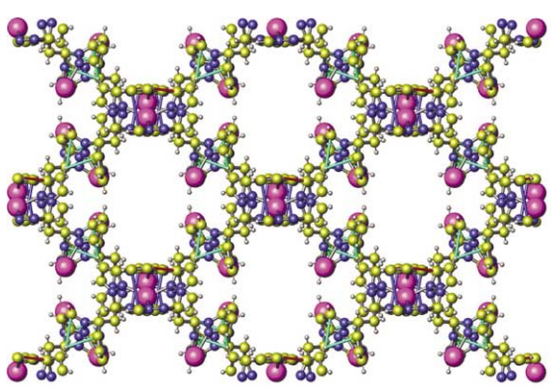

Fig. 7 View of **2·CH$_3$CN** down the *c* axis emphasizing the columnar network of the cations.

Our repeated observations of the cooperative π–π and CH–π interaction between pyrazolyl groups in the above and other metal(pyrazolyl) compounds[4,5] provoked a database search in order to determine whether such an interaction, which we have termed the 'quadruple pyrazolyl embrace', was either found only in isolated examples or was representative of a common framework. The 5.24 version of the Cambridge Structural Database (CSD, November 2002, 272066 entries) was utilized in the search. The C–H bonds were normalized at 1.083 Å and only structures with an *R* factor < 0.1 were considered. In the first step of investigation all $X(pz)_2M$ groups were identified (X = boron or carbon; pz = pyrazolyl group = $C_3H_3N_2$; M = any metal or metalloid bound to a pyrazolyl group nitrogen atom). This search yielded a subset of 679 crystal structures that was used in further analyses. Further restrictions on the database search then followed from the geometric parameters given in Fig. 8 and from accepted values for CH–π and π–π interactions.

Thus, a centroid-to-centroid distance range of 3.0 Å to 4.6 Å along with a dihedral angle, a, range of 0° to 20° was defined to encompass either intra- or inter-molecular π–π stacking interactions involving the pyrazolyl groups. The CH · · · π interaction was allowed to retain a H · · · centroid interval between 2.0 Å and 3.3 Å along with a corresponding CH · · · centroid angle (θ) range between 110 and 180°. As a result of these geometric restrictions, the hydrogen atoms involved in the CH · · · π interactions are always oriented above the π cloud of the corresponding hydrogen-accepting pyrazolyl ring. Therefore, no other parameters were necessary for defining the CH · · · π interaction, as in other cases.[11a] From these combined restraints, 170 crystal structures from the previously obtained subset of 679 or 25% were found to contain a quadruple pyrazolyl embrace. Since some of the entries contained more than one example of such an interaction, these 170 entries generated 204 examples of the motif. The discussion of the geometric parameters associated with this interaction utilizes the 204 examples.

Analysis of the data for the π–π stacking component of the pyrazolyl embrace identified a constrained motif where the three structural parameters that are typically associated with face-to-face arene–arene stacking interaction—the dihedral angle a between the mean planes, the displacement (offset, or slip) angle β formed between the ring–centroid vector and the ring normal to one of the pyrazolyl planes (Fig. 8), and the centroid–centroid distance—each has a narrow range of values within the already truncated search window. Fig. 9 reveals that in a vast majority of examples, the head-to-tail face-to-face stacking between pyrazolyl rings is either coplanar or within a few degrees of coplanarity (a is less than 2° in 82% of the cases and less than 8.5° in 90%); the average dihedral angle between the planes, a_{av}, is 1.8°. In 95% (194/204) of the cases, the stacking between mean planes of pyrazolyl rings is offset by a narrow displacement angle range where β is between 4.2° and 28.3° (Fig. 10). The average displacement angle β_{av} was found to be 16.1°. A majority (183/204, 90%) of the centroid–centroid distances were found in the range between 3.4 Å and 4.0 Å (Fig. 11) where the average distance was 3.71 Å.

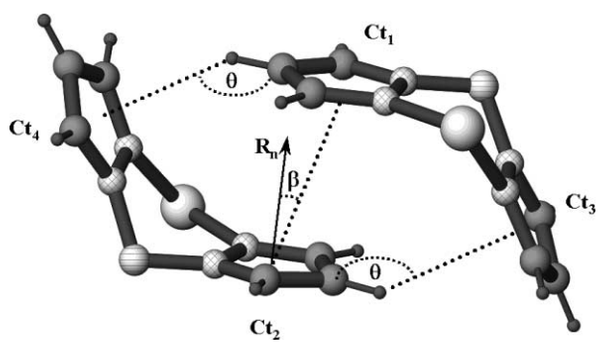

Fig. 8 Geometric parameters associated with the quadruple pyrazolyl embrace: Ct = ring centroid, R_n = ring normal, β = angle between the ring normal and centroid–centroid vector, θ = C–H–Ct angle in C–H · · · π interactions; the Ct_1–Ct_2 distance was constrained to an intra- or inter-molecular (group) contact between 3.0 and 4.6 Å; the dihedral angle between the stacked pyrazolyl rings (a, not pictured here) was allowed to range from 0.0 up to 20.0°; the displacement of the pyrazolyl rings involved in π–π stacking was measured by β, allowed to vary between 0° and 90°. The Ct_3–H and Ct_4–H distances were constrained to an intra- or inter-molecular (group) contact between 2.0 and 3.3 Å, monitoring the θ angle between 110° and 180°; carbon and hydrogen atoms are represented as gray spheres, nitrogen as cross-hatched spheres, boron/carbon as spheres with horizontal line fill and metal/metalloid as large empty spheres.

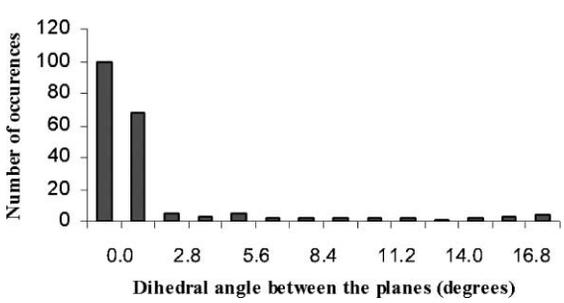

Fig. 9 Distribution in dihedral angle a (°) between mean planes of pyrazolyl rings involved in the π–π interaction.

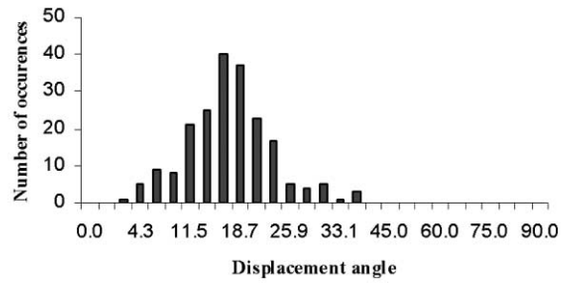

Fig. 10 Histogram of displacement angles β (°) between pyrazolyl planes in the π–π interaction.

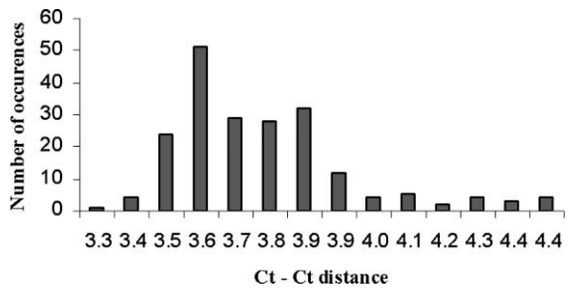

Fig. 11 Histogram for the centroid–centroid distance (Å) between two pyrazolyl rings as outlined in Fig. 8.

Data analysis for the geometry of the CH · · · π interactions in the quadruple pyrazolyl embrace was in agreement with results obtained for other weak hydrogen bonding interactions [*i.e.* CH · · · X (X = O, N, F, C)]; that is, as the CH · · · X (where X in this case is the centroid of the pyrazolyl ring) length decreases, the associated CH–centroid angles approach 180°.[11–13] The scattergram for this interaction in the pyrazolyl embrace is found in Fig. 12. An examination of the H · · · centroid distances (see histogram, Fig. 13) and the data for the associated CH · · · centroid angles (θ) afforded average values of 2.76 Å and θ_{av} of 141.6°, respectively.

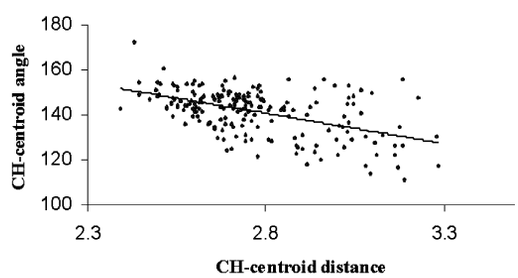

Fig. 12 Scattergram of CH · · · Ct angles (°) *vs.* H · · · Ct distances (Å).

The results of the database search indicate that the π–π and CH–π components of the quadruple pyrazolyl embrace influence the values of each. A low value of β is precluded in metal complexes of poly(pyrazolyl)-methane or -borate ligands by the existence of the CH–π interaction and by the rigidity of the $X(pz)_2M$ units. A large value of β, even one as large as the average displacement angle (β) for N-substituted heterocycles of 27°,[11] is prevented by the attractive nature of the CH–π interaction. The observed average displacement angle β_{av} of 16.1° found in the search for cases of the quadruple pyrazolyl

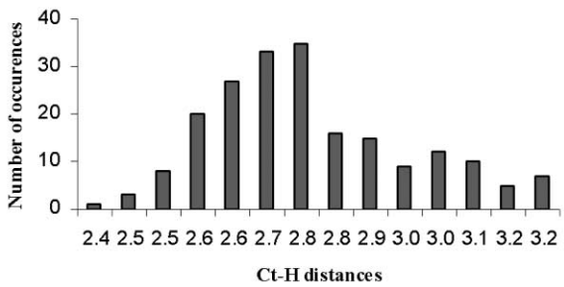

Fig. 13 Histogram of H ··· Ct distances (Å).

embrace is a compromise between the two forces. An ideal CH–π interaction would be such that the donor–hydrogen ··· acceptor angle θ would be 180°, but observed values are always less than this ideal value. Fig. 12 shows that the CH ··· centroid angle increases as the distance decreases, however the trend line has a smaller slope than in other cases [12,13] because of the presence of the π–π stacking between the pyrazolyl rings. This interaction serves to confine the CH ··· centroid angle to an average of 142°.

Conclusions

The first example of an organic-linked bis(pyrazolyl)methane ligand, $CH_2[CH(pz)_2]_2$, is reported here, thereby filling a void in the known family of linked poly(pyrazolyl)methane ligands. Two silver complexes of this ligand have been characterized in solution and in the solid state by single crystal X-ray diffraction studies. The triflate salt forms a discrete dimeric dication in which two ligands sandwich two silver cations forming a bicyclic sixteen-membered ring system. The nitrate forms a trimetallic complex with overall a 2 : 3 mol ratio of ligand to metal. In each case, the organic ligand participates in multiple noncovalent interactions that associate the multimetallic 'cationic cores' in the solid state into supramolecular structures. In both cases, the cationic centers were associated by cooperative π–π and CH–π interactions. This combined set of interactions has been entitled the *quadruple pyrazolyl embrace*. A search of the crystallographic database showed that this interaction is relatively common for metal complexes of simple poly(pyrazolyl)-methanes or -borates and occurs in a quarter of all cases. At its simplest level, such an interaction between $X(pz)_2M$ units will yield discrete dimeric species. Higher dimensionality materials may be obtained by covalently linking bis(pyrazolyl)methane units as exemplified by the silver complexes of tetrakis(pyrazolyl)propane described here. While the data contained within this paper serves to demonstrate the viability of the pyrazolyl embrace as a synthon for the construction of supramolecular edifices, certainly the crystal structure of $[Ag_3\{CH_2[CH(pz)_2]_2\}_2](NO_3)_3(CH_3CN)_3$ serves as a useful example of the importance of other noncovalent interactions (weak hydrogen bonds) in the organization of species containing poly(pyrazolyl)-methane and -borate ligands in the solid state. It should be emphasized that the existence of $X(pz)_2M$ units within a chemical species is insufficient to guarantee that a pyrazolyl embrace will be observed, as the framework was found in only 25% of the structurally characterized cases. The factors that influence the presence or absence of the quadruple pyrazolyl embrace as well as the influence of substituents on the geometry of the pyrazolyl embrace will be adressed in future publications.

Experimental

General comments

All manipulations involving uncomplexed silver salts were carried out either in the drybox under a purified N_2 atmosphere or by using standard Schlenk techniques where solvents were commercially available, purified by conventional means, and distilled immediately prior to use. Silica gel (230–400 mesh, 40–63 μm) was purchased from Fisher Scientific. Silver salts, pyrazole (Hpz), and all other organic reagents were used as purchased from Aldrich. Robertson Microlit Laboratories, Inc. (Madison, NJ) performed the elemental analyses. Samples for melting point determinations were contained in flame sealed capillaries and the reported temperatures are uncorrected. The NMR spectra were recorded by using a Varian Mercury 400 instrument. Chemical shifts are reported in ppm and were referenced to the solvent resonances as internal standards. Mass spectrometric measurements were obtained on a JEOL JMS-AX505HA spectrometer.

Syntheses

$CH_2[CH(pz)_2]_2$, 1,1′,3,3′-tetrakis(1-pyrazolyl)propane. A 100 mL Schlenk flask fitted with a magnetic stirbar was charged with 5.5 mL (0.033 mol) of malonaldehyde dimethylacetal, 9.3 g (0.14 mol) of pyrazole, and 0.050 g (0.26 mmol) of *p*-toluenesulfonic acid monohydrate. The flask was attached to a short path distillation apparatus that was connected to a tared vial (to monitor MeOH evolution) and the mixture was heated with an external heating mantle until approximately 5 mL of methanol (theoretical 5.4 mL) had been collected (10 h). After the reaction mixture had been cooled to room temperature, 50 mL each of CH_2Cl_2 and H_2O were added. The aqueous portion was extracted with three 50 mL portions of CH_2Cl_2, the combined organic fractions were dried over $MgSO_4$, filtered and solvent was removed to leave a brown oily solid. The solid was taken up in methylene chloride and flushed through a plug of silica to give $CH_2[CH(pz)_2]_2$ as a colorless solid. Recrystallization from Et_2O provided 5.4 g (53% yield) of $CH_2[CH(pz)_2]_2$ as colorless plates. mp, 92–93 °C. Anal. Calcd. (Obs.) for $C_{15}H_{16}N_8$: C, 58.43 (58.33) H, 5.23 (5.08); N, 36.34 (36.17%). ^{1}H NMR (400 MHz, $CDCl_3$): δ 7.58 (d, J = 1 Hz, 4 H, H_5-pz), 7.54 (d, J = 2 Hz, 4H, H_3-pz), 6.29 (dd, J = 2, 1 Hz, 4H, H_4-pz), 6.17 (t, J = 8 Hz, 2H, $CH(pz)_2$), 3.93 (t, J = 8 Hz, 2H, CH_2). ^{1}H NMR (400 MHz, acetone-d_6): δ 7.83 (d, J = 2 Hz, 4 H, H_3-pz), 7.53 (d, J = 1 Hz, 4H, H_5-pz), 6.31 (m, 4H, H_4-pz), 6.29 (t, J = 8 Hz, 2H, $CH(pz)_2$), 4.02 (t, J = 8 Hz, 2H, CH_2). ^{13}C NMR (101.62 MHz, $CDCl_3$): δ 140.9 (C_5-pz), 129.1 (C_3-pz), 107.2 (C_4-pz), 71.9 (CH-pz), 38.4 (CH_2). ^{13}C NMR (101.62 MHz, acetone-d_6): δ 140.9 (C_5-pz), 130.0 (C_3-pz), 107.2 (C_4-pz), 72.5 (CHpz), 38.0 (CH_2). HRMS: Direct probe (*m*/*z*): $[M - H]^+$ calcd for $C_{15}H_{16}N_8$, 308.1498; found, 308.1500. Direct probe MS *m*/*z* (Rel. Int. %) [assgn]: 308 (10) $[M]^+$, 240 (53) $[M - Hpz]^+$, 173 (85) $[M - 2Hpz]^+$, 147 (87) $[HC(pz)_2]^+$, 105 (100) $[M - 3Hpz]^+$, 81 (25) $[HCpz]^+$, 69 (37) $[H_2pz]^+$.

$[Ag_2\{\mu\text{-}CH_2[CH(pz)_2]\}_2](SO_3CF_3)_2$ (1). A solution of 0.26 g (1.0 mmol) of $Ag(O_3SCF_3)$ in 10 mL THF was added by cannula to a foil-covered 50 mL Schlenk flask that contained a solution of 0.31 g (1.0 mmol) of $CH_2[CH(pz)_2]_2$ in 10 mL THF. After the reaction mixture had been magnetically stirred for 14 h at room temperature, the soluble and insoluble portions were separated by cannula filtration. The insoluble portion was washed with two 5 mL portions of Et_2O and was dried under vacuum to leave 0.23 g (40% yield) of the product as an analytically pure colorless powdery solid. After the mother liquor from the initial separation had been concentrated to ¼ volume, an additional 0.22 g of product was isolated by cannula filtration, washing with Et_2O and drying under vacuum as above. The total isolated yield was 0.45 g (79%); mp 246–250 °C decomp. Anal. Calcd. (found) for $C_{16}H_{16}N_8F_3O_3SAg$: C, 34.00 (33.78); H, 2.85 (2.45); N, 19.82 (19.64%). ^{1}H NMR (400 MHz, acetone-d_6): δ 8.14 (d, J = 2 Hz, 4 H, H_3-pz), 7.73 (d, J = 1 Hz, 4H, H_5-pz), 7.70 (t, J = 8 Hz, 2H, $CH(pz)_2$), 6.39 (dd, J = 2, 1 Hz, 4H, H_4-pz), 4.74 (t, J = 8 Hz, 2H, CH_2). ^{13}C NMR (101.62 MHz, acetone-d_6): δ 144.3 (C_5-pz), 133.5 (C_3-pz), 107.2 (C_4-pz),

71.7 (CHpz), 38.4 (CH_2). HRMS: Direct probe (*m*/*z*): calcd for $C_{31}H_{32}N_{16}F_3O_3SAg_2$, $[Ag_2L_2OTf]^+$, 979.0618; found, 979.0629; calcd for $C_{30}H_{32}N_{16}Ag$, $[AgL_2]^+$, 723.2047; found, 723.2032. ESI(+) MS *m*/*z* (Rel. Int. %) [assgn]: 981 (8) $[Ag_2L_2OTf]^+$, 723 (25) $[AgL_2]^+$, 415 (100) $[AgL]^+$, 349 (27) [AgL − Hpz]. Recrystallization of the colorless solid by vapor diffusion of Et_2O into either CH_3CN or acetone solutions of the compound afforded colorless crystalline blocks of $[Ag_2\{\mu\text{-}CH_2[CH(pz)_2]\}_2](SO_3CF_3)_2$ suitable for single crystal X-ray diffraction.

$[Ag_3\{\mu\text{-}CH_2[CH(pz)_2]_2\}_2](NO_3)_3(CH_3CN)_2$, (2). A solution of 0.17 g (1.0 mmol) of $Ag(NO_3)$ in 10 mL CH_3CN was added by cannula to a foil-covered 50 mL Schlenk flask that contained a solution of 0.31 g (1.0 mmol) of $CH_2[CH(pz)_2]_2$ in 10 mL THF. After the reaction mixture had been magnetically stirred for 30 min at room temperature, the solvent was removed by cannula filtration to leave a colorless solid. The solid was washed with two 5 mL portions of acetonitrile and then was dried under vacuum to leave 0.39 g (96% based on $CH_2[CH(pz)_2]_2$) of analytically pure $[Ag_3\{\mu\text{-}CH_2[CH(pz)_2]_2\}_2](NO_3)_3(CH_3CN)_2$ as microcrystalline needles. mp 225–230 °C decomp. to orange glass. Anal. Calcd. (found) for $C_{34}H_{38}N_{21}O_9Ag_3$: C, 33.79 (33.72); H, 3.17 (2.94); N, 24.34 (24.05%). ^{1}H NMR (400 MHz, acetone-d_6): δ 8.05 (d, J = 2 Hz, 4 H, H_3-pz), 7.69 (d, J = 1 Hz, 4H, H_5-pz), 7.30 (t, J = 8 Hz, 2H, $CH(pz)_2$), 6.39 (dd, J = 2, 1 Hz, 4H, H_4-pz), 4.50 (t, J = 8 Hz, 2H, CH_2). ^{1}H NMR (400 MHz, CD_3CN): δ 7.75 (d, J = 1 Hz, 4 H, H_5-pz), 7.57 (d, J = 2 Hz, 4H, H_3-pz), 6.50 (br m, 2H, $CH(pz)_2$), 6.31 (dd, J = 2, 1 Hz, 4H, H_4-pz), 4.14 (t, J = 7 Hz, 2H, CH_2). ^{13}C NMR (101.62 MHz, CD_3CN): δ 142.7 (C_5-pz), 131.8 (C_3-pz), 107.8 (C_4-pz), 71.7 (CHpz), 37.9 (CH_2). ESI(+) MS *m*/*z* (Rel. Int. %) [assgn]: 1061 (1) $[Ag_3L_2(NO_3)_2]^+$, 894 (2) $[Ag_2L_2(\text{acetone-}d_6)]^{2+}$, 723 (50) $[AgL_2]^+$, 456 (100) $[AgL(CH_3CN)]$, 415 (62) $[AgL]^+$. Recrystallization of the colorless solid by vapor diffusion of Et_2O into a CH_3CN solution of the compound afforded colorless needles of the acetonitrile tri-solvate complex **2·CH_3CN** suitable for a single crystal X-ray diffraction study.

Crystal structure determinations

A colorless block of each of **1** and **2·CH_3CN** was mounted onto the end of a thin glass fiber using inert oil. X-Ray intensity data covering the full sphere of reciprocal space were measured at 220.0(2) K for **1** and at 150.0(2) K for **2·CH_3CN** on a Bruker SMART APEX CCD-based diffractometer (Mo-Kα radiation, λ = 0.71073 Å).[14] The raw data frames were integrated with SAINT+,[14] which also applied corrections for Lorentz and polarization effects. The final unit cell parameters are based on the least-squares refinement of 7613 reflections from the data set of **1** and on the refinement of 6032 reflections from the data set of **2·CH_3CN** each with $I > 5\sigma(I)$. Analysis of the data for each showed negligible crystal decay during collection. Both data sets were corrected for absorption effects with SADABS.[15]

Crystal data for 1. $[Ag_2\{\mu\text{-}CH_2[CH(pz)_2]\}_2](SO_3CF_3)_2$ crystallizes in the triclinic system. The structure was solved in the space group $P\bar{1}$ by a combination of direct methods and difference Fourier syntheses, and refined by full-matrix least-squares against F^2, using SHELXTL.[15] The $[Ag_2\{\mu\text{-}CH_2[CH(pz)_2]\}_2]^{2+}$ complex resides on a center of symmetry. The triflate anion is disordered over two nearby positions in the ratio 60 : 40 and was refined with the aid of seven geometric restraints. All non-hydrogen atoms were refined with anisotropic displacement parameters; hydrogen atoms were placed in geometrically idealized positions and included as riding atoms with refined isotropic displacement parameters.

$C_{32}H_{32}Ag_2F_6N_{16}O_6S_2$, M = 1130.60, triclinic, a = 9.8259(5), b = 10.4688(5), c = 12.3726(6) Å, α = 96.8090(10)°, β = 111.2290(10)°, γ = 107.9600(10)°. U = 1089.84(9) Å^3, Z = 1, μ(Mo-Kα) = 1.082 mm^{-1}, 9992 reflections measured, 4444 unique (R_{int} = 0.0228) which were used in all calculations. The final $wR(F^2)$ was 0.0696 (all data).

Crystal data for 2·CH_3CN. Systematic absences in the intensity data for **2·CH_3CN** were consistent with the space groups *Cc* and *C*2/*c*; intensity statistics indicated centricity. The structure was solved in *C*2/*c* by a combination of direct methods and difference Fourier syntheses, and refined by full-matrix least-squares against F^2, using SHELXTL.[15] The asymmetric unit contains two crystallographically inequivalent Ag centers, Ag1 and Ag2. Ag1 is located on a two-fold axis of rotation. The crystallographically imposed C_2 symmetry is incompatible with the true symmetry of the complex (none) and generates disorder about the Ag2 center. One Ag2 coordination site is occupied by ½ NO_3^- and ½ CH_3CN. Both disorder components were clearly located in the difference map and freely refined with anisotropic displacement parameters. Occupation factors initially refined to near ½ and were subsequently fixed at that value to satisfy charge balance. Two additional uncoordinated CH_3CN molecules of crystallization were located, one in the vicinity of Ag2 and another disordered over four positions. The latter was refined with fixed occupation and temperature factors; hydrogen atoms were not located or calculated. All other non-hydrogen atoms were refined with anisotropic displacement parameters. Defined hydrogen atoms were placed in geometrically idealized positions and included as riding atoms. Refinement in *Cc* resulted in the same NO_3^-/CH_3CN disorder as well as large correlations between symmetry-related atoms, therefore *C*2/*c* was retained as the proper space group.

$C_{36}H_{41}Ag_3N_{22}O_9$, M = 1249.52, monoclinic, a = 21.7230(15), b = 14.9693(10), c = 14.8892(10) Å, $\alpha = \gamma$ = 90, β = 94.9640(10)°. U = 4823.5(6) Å^3, Z = 4, μ(Mo-Kα) = 1.281 mm^{-1}, 16502 reflections measured, 4259 unique (R_{int} = 0.0300) which were used in all calculations. The final $wR(F^2)$ was 0.0987 (all data).

CCDC reference numbers 204327 and 204328.

See http://www.rsc.org/suppdata/dt/b3/b301635h/ for crystallographic data in CIF or other electronic format.

Acknowledgements

We thank the National Science Foundation (CHE-0110493) for support. The Bruker CCD Single Crystal Diffractometer was purchased using funds provided by the NSF Instrumentation for Materials Research Program through Grant DMR:9975623.

References and notes

1 (*a*) Y. Cui, H. L. Ngo, P. S. White and W. Lin, *Inorg. Chem.*, 2003, **42**, 652; (*b*) S. J. Lee, A. Hu and W. Lin, *J. Am. Chem. Soc.*, 2002, **124**, 12948; (*c*) B. Xing, M.-F. Choi and B. Xu, *Chem. Eur. J.*, 2002, **8**, 5028; (*d*) O. R. Evans, H. L. Ngo and W. Lin, *J. Am. Chem. Soc.*, 2001, **123**, 10395.

2 (*a*) F. P. Gabbaï, *ACS Symp. Ser.*, 2002, **822**, 118–130; (*b*) M. Tsunoda and F. P. Gabbaï, *J. Am. Chem. Soc.*, 2000, **122**, 8335; (*c*) J. R. Gardinier and F. P. Gabbaï, *J. Chem. Soc., Dalton Trans.*, 2000, 2861; (*d*) M. Tschinkl, A. Schier, J. Riede and F. P. Gabbaï, *Angew. Chem., Int. Ed.*, 1999, **38**, 3547.

3 (*a*) M. Shibasaki and M. Kanai, *Chem. Pharm. Bull.*, 2001, **49**, 511; (*b*) W. E. Piers, G. J. Irvine and V. C. Williams, *Eur. J. Inorg. Chem.*, 2000, 2131; (*c*) Y. Chen, R. Kiattansakul, B. Ma and J. K. Snyder, *J. Org. Chem.*, 2001, **66**, 6932; (*d*) K. Nozaki, K. Kobori, T. Uemura, T. Tsutsumi, H. Takaya and T. Hiyama, *Bull. Chem. Soc. Jpn.*, 1999, **72**, 1109; (*e*) L. B. Fields and E. N. Jacobsen, *Tetrahedron: Asymmetry*, 1993, **4**, 2229.

4 (*a*) D. L. Reger, T. D. Wright, R. F. Semeniuc, T. C. Grattan and M. D. Smith, *Inorg. Chem.*, 2001, **40**, 6212; (*b*) D. L. Reger, R. F. Semeniuc and M. D. Smith, *J. Chem. Soc., Dalton Trans.*, 2002, 476; (*c*) D. L. Reger, R. F. Semeniuc and M. D. Smith, *J. Organomet. Chem.*, 2003, **666**, 87; (*d*) D. L. Reger, K. J. Brown and M. D. Smith, *J. Organomet. Chem.*, 2002, **658**, 50.

5 D. L. Reger, R. F. Semeniuc and M. D. Smith, *Inorg. Chem.*, 2001, **40**, 6545.

6 (*a*) D. L. Reger, R. F. Semeniuc and M. D. Smith, *Eur. J. Inorg. Chem.*, 2002, 543; (*b*) D. L. Reger, R. F. Semeniuc and M. D. Smith, *Inorg. Chem. Commun*, 2002, **5**, 278.
7 (*a*) D. A. McMorran and P. J. Steel, *Inorg. Chem. Commun.*, 2003, **6**, 43–47; (*b*) D. A. McMorran, S. Pfadenhauer and P. J. Steel, *Aust J. Chem.*, 2002, **55**, 519; (*c*) S. Alves, A. Paulo, J. D. G. Correia, A. Domingos and I. Santos, *J. Chem. Soc., Dalton Trans.*, 2002, 4714; (*d*) J. M. Holland, S. A. Barrett, C. A. Kilner and M. A. Halcrow, *Inorg. Chem. Commun.*, 2002, **5**, 328; (*e*) A. M. Schuitema, M. Engelen, I. A. Koval, S. Gorter and W. L. Driessen, *Inorg. Chim. Acta*, 2001, **324**, 57; (*f*) J. C. Tao, Y.-J. Wu and J.-Y. Song, *Polyhedron*, 1999, **18**, 1015; (*g*) K. L. V. Mann, J. C. Jeffery, J. A. McCleverty and M. D. Ward, *J. Chem. Soc., Dalton Trans.*, 1998, 3029; (*h*) A. Jacobi, G. Huttner, U. Winterhalter and S. Cunskis, *Eur. J. Inorg. Chem.*, 1998, 675.
8 While the sextuple phenyl embrace is the most common supramolecular framework involving PPh_3 units (see I. Dance and M. Scudder, *J. Chem. Soc., Dalton Trans.*, 2000, 1587 and references therein), the quadruple phenyl embrace and other interactions involving the phenyl groups are important for the PPh_4 cation (see I. Dance and M. Scudder, *Chem. Eur. J.*, 1996, **2**, 481).
9 (*a*) A. Rohrer, R. Ocampo and H. J. Callot, *Synthesis*, 1994, **9**, 923; (*b*) P. Gosselin, F. Rouessac and H. Zamarlik, *Bull. Soc. Chim. Fr.*, 1981, **5–6**, 192; (*c*) K. C. Brannock, *J. Org. Chem.*, 1960, **25**, 258.
10 C. Janiak, *J. Chem. Soc., Dalton Trans.*, 2000, 3885 and references therein.
11 (*a*) H. Takahashi, S. Tsuboyama, Y. Umezawa, K. Honda and M. Nishio, *Tetrahedron*, 2000, **56**, 6185–6191; (*b*) M. Nishio, M. Hirota and Y. Umezawa, *The CH/π interaction Evidence, Nature and Consequences*, Wiley-VCH, New York, 1998; (*c*) S. Tsuzuki, K. Honda, T. Uchimaru, M. Mikami and K. Tanabe, *J. Am. Chem. Soc.*, 2000, **122**, 11450–11458.
12 T. Steiner, *Angew. Chem., Int. Ed.*, 2002, **41**, 48.
13 D. Braga, F. Grepioni and E. Tedesco, *Organometallics*, 1998, **17**, 2669.
14 SMART Version 5.625, SAINT+ Version 6.02a and SADABS, Bruker Analytical X-ray Systems, Inc., Madison, WI, 1998.
15 G. M. Sheldrick, SHELXTL Version 5.1, Bruker Analytical X-ray Systems, Inc., Madison, WI, 1997.